spectrometry allows convenient characterization of intact conjugates and contributed significantly to the identification of this metabolite. MX and its major hydroxyl metabolites are usually extracted from biological samples under alkaline conditions, because of their pK_a values, and then quantified by HPLC analysis by using acidified eluents. In this study, the pH of the mobile phase for HPLC analysis and HPLC separation before the mass analysis was set at 7.0 to avoid degradation of the carbamoyl moiety in the analyte. Consequently, the $[M-H]^-$ ion of the isolated MX glucuronide was detected at m/z 398, equal to that of MX-glucuronide plus a carbonyloxy moiety. The CID product ion at m/z 193, derived from $[M-H]^-$ suggested the presence of a glucuronic acid moiety in the structure (figure 2B). The molecular mass of the conjugate was further confirmed in the positive-ion chromatogram by the presence of the ion adduct $[M+NH_4]^+$ at m/z 417. The observation of product ions at m/z 224 and 180 further supported the presence of a carbonyloxy moiety. The nucleophilic reaction of the methoxyl group with MX glucuronide resulted in the formation of *N*-methoxycarbonyl-mexiletine, which would not be expected from either *N*-hydroxyglucuronide or *N*-glucuronide. These results support our postulation that the isolated MX glucuronide has the *N*-carbonyloxy β-D-glucuronide structure. Although quantification by a validated analytical method has not yet been performed, the estimated amounts of the isolated glucuronide corresponded to about 80% of total MX glucuronide, as calculated from the increase of MX after acid hydrolysis of the urinary metabolite. Assuming that around 30% of orally administered MX is excreted as MX glucuronide in urine (Abolfathi *et al.* 1993), the urinary recovery of MX carbonyloxy-β-D-glucuronide is expected to account for over 25% of the dose. Therefore, this novel glucuronide appears to be one of the major metabolites of MX in human urine.

Crooks and Donnellan (1989) demonstrated that amine carbamates were formed in a single step from unprotonated primary or secondary aliphatic amines and CO_2 in the presence of H_2O as a catalyst. This reaction can readily occur in physiological type media, such as the carbon dioxide/bicarbonate buffer system (Myers and Nelson 1990) and also plays important roles in biological systems. For example, carbamic acid is formed during the transport of carbon dioxide by haemoglobin and is associated with the physiological reactions of a number of other proteins and peptides (Kilmartin and Rossi-Bernardi 1973, Gros *et al.* 1981). There are only a few reports on carbamate metabolites of drugs containing a primary amino group. *N*-Carbonyloxy-β-D-glucuronides of an antiarrhythmic agent, tocainide, and an antiviral agent, rimantadine, have been reported to be excreted in urine after oral administration of these drugs (Elvin *et al.* 1980, Brown *et al.* 1990, Kwok *et al.* 1990). The formation of the *N*-carbonyloxy-β-D-glucuronide conjugate of MX is likely to involve initial reversible addition of CO_2 to the primary amine function to form a carbamic acid intermediate, which is in turn glucuronidated to form a stable carbonyloxy-β-D-glucuronide conjugate. The formation of carbamoyl conjugates via carbamic acid intermediates may be quite common with amines, but would have been unnoticed because of the instability of the intermediates.

Regarding carvedilol and mofegilin, Schaefer (1992) and Dow *et al.* (1994) reported that the carbamate glucuronide was observed in urine and in a reaction mixture containing dog or human liver microsomes together with uridine diphosphoglucuronic acid (UDPGA) in carbonate buffer. They showed that incubation

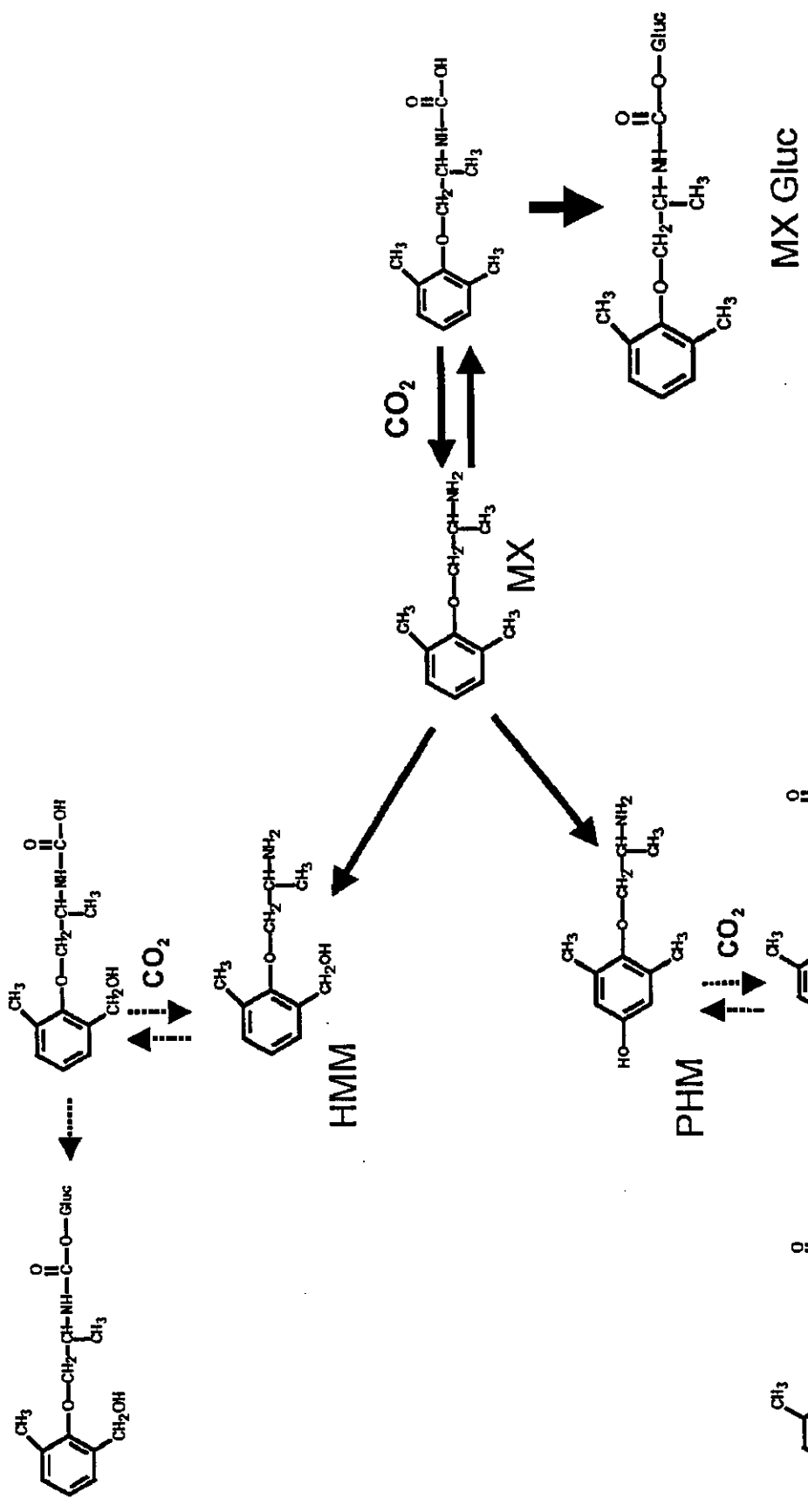

Figure 7. Proposed metabolic pathways of glucuronic acid conjugation of MX in man. Dotted lines express the possible metabolic pathways suggested by the results of this study.

in bicarbonate buffer spiked with UDPGA under a CO_2 atmosphere was necessary for the maximum formation of the carbamoyl glucuronide conjugate with hepatic microsomes. Interestingly, in our preliminary *in vitro* glucuronidated study of MX, 4HM, 2HM and NHM using a standard method without a CO_2 source, it was observed that NHM gave the *N*-hydroxyglucuronide, whereas the amounts of MX, 4HM and 2HM were unchanged after incubation, and no relevant product was detected on the chromatogram. Hence, it can be speculated that 4HM and 2HM are also conjugated with glucuronic acid following the formation of carbamic acid intermediates, because an amino moiety is present in both 4HM and 2HM, as well as MX. In summary, it is proposed that the metabolic pathways of glucuronic acid conjugation of MX in human are as shown in figure 7. The methanolysis reaction described here might be a generally useful method for the characterization of carbonyloxy glucuronides because the resulting methyl carbamate product was stable and could be determined by HPLC analysis.

The present results suggest that MX glucuronide was predominantly formed via non-enzymatic carboxylation followed by enzymatic glucuronidation. This compound had a different chemical structure to that proposed by Turgeon *et al.* (1992), who suggested that the major conjugated metabolite of MX observed in rabbits and humans was the conjugate of *N*-hydroxymexiletine. The latter authors proposed that this NHM glucuronide was hydrolysed to give MX *per se*. To test their hypothesis, NHM glucuronide was chemically synthesized in the authors' laboratory by the same method described in their paper, on a milligram scale. In the HPLC analysis of the reaction mixture after enzymatic hydrolysis of NHM glucuronide, NHM but not MX was detected.

In conclusion, a novel MX glucuronide was isolated from human urine and it was established that the metabolite contained a carboxyl moiety in its structure by using LC/MS/MS and HPLC under neutral conditions. The estimated recovery of mexiletine carbonyloxy β-D-glucuronide corresponded to over 25% of the dose of MX indicating that it is a major component of MX glucuronide in urine.

Acknowledgements

The authors thank Mr M. Kubota of ThermoQuest for the mass spectral analysis of the purified compound.

References

ABOLFATHI, Z., FISET, C., GILBERT, M., MOERIKE, K., BELANGER, P. M. and TURGEON, J., 1993, Role of polymorphic debrisoquin 4-hydroxylase activity in the stereoselective disposition of mexiletine in humans. *Journal of Pharmacology and Experimental Therapeutics*, **266**, 1196–1201.

BECKETT, A. H. and CHIDOMERE, E. C., 1977, The identification and analysis of mexiletine and its metabolic products in man. *Journal of Pharmacy and Pharmacology*, **29**, 281–285.

BROLY, F., VANDAMME, N., LIBERSA, C. and LHERMITTE, M., 1991, The metabolism of mexiletine in relation to the debrisoquine/spartein-type polymorphism of drug oxidation. *British Journal of Clinical Pharmacology*, **32**, 459–466.

BROWN, S. Y., GARLAND, W. A. and FUKUDA, E. K., 1990, Isolation and characterization of an unusual glucuronide conjugate of rimantadine. *Drug Metabolism and Disposition*, **18**, 546–547.

CAMPBELL, N. P. S., KELLY, J. G., ADGEY, A. A. J. and SHANKS, R. G., 1978, The clinical pharmacology of mexiletine. *British Journal of Clinical Pharmacology*, **6**, 103–108.

CROOKS, J. E. and DONNELLAN, J. P., 1989, Kinetics and mechanism of the reaction between carbon dioxide and amines in aqueous solution. *Journal of the Chemical Society Perkin Transactions*, **2**, 331–333.

Dow, J., Piriou, F., Wolf, E., Dulery, B. D. and Haegele, K. D., 1994, Novel carbamate metabolites of mofegiline, a primary amine monoamine oxidase B inhibitor, in dogs and humans. *Drug Metabolism and Disposition*, **22**, 738–749.

Elvin, A. T., Keenaghan, J. B., Byrnes, E. W., Tenthorey, P. A., Mcmaster, P. D., Takman, B. H., Lalka, D., Meyer, M. B. and Ronfeld, R. A., 1980, Tocainide conjugation in humans: novel biotransformation pathway for a primary amine. *Journal of Pharmaceutical Sciences*, **69**, 47–49.

Gros, G., Rollema, H. S. and Forster, R. E., 1981, The carbamate equilibrium of α- and ε-amino groups of human haemoglobin at 37°C. *Journal of Biological Chemistry*, **256**, 5471–5480.

Haeselbarth, V., Doevendans, J. E. and Wolf, M., 1981, Kinetics and bioavailability of mexiletine in healthy subjects. *Clinical Pharmacological Therapy*, **29**, 729–736.

Kilmartin, J. V. and Rossi-Bernardi, L., 1973, Interaction of hemoglobin with hydrogen ions, carbon dioxide, and organic phosphates. *Physiological Review*, **53**, 836–890.

Kwok, D. W. K., Pillai, G., Vaughan, R., Axelson, J. E. and McErlane, K. M., 1990, Preparative high-performance liquid chromatography and preparative thin-layer chromatography isolation of tocainide carbamoyl-*O*-β-d-glucuronide: Structural characterization by gas chromatography-mass spectrometry and fast atom bombardment-mass spectrometry. *Journal of Pharmaceutical Sciences*, **79**, 857–861.

Lledo, P., Abrams, S. M. L., Johnston, A., Patel, M., Pearson, R. M. and Turner, P. 1993, Influence of debrisoquine hydroxylation phenotype on the pharmacokinetics of mexiletine. *European Journal of Clinical Pharmacology*, **44**, 63–67.

Murray, K. T., Barbey, J. T., Kopelman, H. A., Siddoway, L. A., Echt, D. S., Woosley, R. L. and Roden, D. M., 1989, Mexiletine and tocainide: a comparison of antiarrhythmic efficacy, adverse effects and predictive value of lidocaine testing. *Clinical Pharmacological Therapy*, **45**, 553–561.

Myers, T. G. and Nelson, S. D., 1990, Neuroactive carbamate adducts of β-N-methylamino-L-alanine and ethylenediamine. *Journal of Biological Chemistry*, **265**, 10193–10195.

Nakajima, M., Kobayashi, K., Shimada, N., Tokudome, S., Yamamoto, T. and Kuroiwa, Y., 1998, Involvement of CYP1A2 in mexiletine metabolism. *British Journal of Clinical Pharmacology*, **46**, 55–62.

Pentikainen, P. J., Halinen, M. O. and Helin, M. J., 1983, Pharmacokinetics of oral mexiletine in patients with acute myocardial infarction. *European Journal of Clinical Pharmacology*, **25**, 773–777.

Prescott, L. F., Pottage, A. and Clements, J. A., 1977, Absorption, distribution and elimination of mexiletine. *Postgraduate Medical Journal*, **53**, 50–55.

Schaefer, W. H., 1992, Formation of a carbamoyl glucuronide conjugate of carvedilol in vitro using dog and rat liver microsomes. *Drug Metabolism and Disposition*, **20**, 130–133.

Senda, C., Yamaura, Y., Kobayashi, K., Fuji, H., Minami, H., Sasaki, Y., Igarashi, T. and Chiba, K., 2001, Influence of the *CYP2D6*10* allele on the metabolism of mexiletine by human liver microsomes. *British Journal of Clinical Pharmacology*, **52**, 100–103.

Turgeon, J., Fiset, C., Giguere, R., Gilbert, M., Moerike, K., Rouleau, J. R., Kromer, H. K., Eichelbaum, M., Grech-Belanger, O. and Belanger, P. M., 1991, Influence of debrisoquine phenotype and of quinidine on mexiletine disposition in man. *Journal of Pharmacology and Experimental Therapeutics*, **259**, 789–798.

Turgeon, J., Pare, J. R. J., Lalande, M., Grech-Belanger, O. and Belanger, P. M., 1992, Isolation and structural characterization by spectroscopic methods of two glucuronide metabolites of mexiletine after N-oxidation and deamination. *Drug Metabolism and Disposition*, **20**, 762–769.

Ueno, K., Tamamura, A., Matsumoto, K., Komamura, K., Kamakura, S., Miyatake, K. and Shibakawa, M., 2002, Evaluation of mexiletine clearance in a Japanese population. *Annals of Pharmacotherapy*, **36**, 241–245.

Available online at www.sciencedirect.com
SCIENCE DIRECT®
Life Sciences 73 (2003) 3201–3212
Life Sciences
www.elsevier.com/locate/lifescie

Metabolism of medroxyprogesterone acetate (MPA) via CYP enzymes in vitro and effect of MPA on bleeding time in female rats in dependence on CYP activity in vivo

Nobuhito Mimura[a], Kaoru Kobayashi[a,*], Yoshika Nakamura[a], Noriaki Shimada[b], Masakiyo Hosokawa[a], Kan Chiba[a]

[a] *Laboratory of Pharmacology and Toxicology, Graduate School of Pharmaceutical Sciences, Chiba University, Yayoi-cho 1-33, Inage-ku, Chiba 263-8522, Japan*
[b] *Daiichi Pure Chemicals, Co., Ltd., Japan*

Received 24 January 2003; accepted 27 May 2003

Abstract

Medroxyprogesterone acetate (MPA) is a drug commonly used in endocrine therapy for advanced breast cancer, although it is known to cause thrombosis as a serious side effect. Recently, we found that cytochrome P450 3A4 (CYP3A4) mainly catalyzed the metabolism of MPA via CYP in human liver microsomes. However, the metabolic products of MPA in humans and rats have not been elucidated. In addition, it is not clear whether thrombosis could be induced by MPA itself or by its metabolites. In this study, we determined the overall metabolism of MPA as the disappearance of the parent drug from an incubation mixture, and identified the enzymes catalyzing the metabolism of MPA via CYP in rats. Moreover, the effects of CYP-modulators on MPA-induced hypercoagulation in vivo were examined. Intrinsic clearance of MPA in rat liver microsomes was increased by treatment with CYP3A-inducers. The intrinsic clearance of MPA in liver microsomes of rats treated with various CYP-inducers showed a significant correlation with CYP3A activity, but not CYP1A activity, CYP2B activity or CYP2C contents. Among the eight recombinant rat CYPs studied, CYP3A1, CYP3A2 and CYP2A2 catalyzed the metabolism of MPA. However, since CYP3A2 and CYP2A2 are male-specific isoforms, CYP3A1 appears to be mainly involved in the metabolism of MPA in liver microsomes of female rats. In an in vivo study, pretreatment of female rats with SKF525A, an inhibitor of CYPs including CYP3A1, significantly ($p < 0.05$) enhanced MPA-induced hypercoagulation, whereas pretreatment with phenobarbital, an inducer of CYPs including CYP3A1, reduced it. These findings suggest that CYP-catalyzed metabolism of MPA is mainly

* Corresponding author. Tel./fax: +81-43-290-2921.
E-mail address: kaoruk@p.chiba-u.ac.jp (K. Kobayashi).

0024-3205/$ - see front matter
doi:10.1016/j.lfs.2003.05.004

catalyzed by CYP3A1 and that MPA-induced hypercoagulation is predominantly caused by MPA itself in female rats.

Keywords: MPA; P450; Rat liver microsomes; cDNA-expression system; Hypercoagulation

Introduction

Medroxyprogesterone acetate (MPA) is one of the drugs most commonly used in endocrine therapy for advanced or recurrent breast cancer and endometrial cancer. However, it is known that MPA can cause serious adverse effects such as thrombosis as well as other side effects such as weight gain, hypertension, nausea and cushingoid effects (Etienne et al., 1992). Although a higher frequency of toxicity has been seen at higher doses (Etienne et al., 1992), it is not clear whether MPA actually contributes to the occurrence of thrombosis, because thrombosis is caused by many factors, including tumors, surgery and genetic mutations of some coagulation factors (Rosendaal, 1999). Recently, it has been reported that MPA shortened bleeding time in rats in a dose-dependent manner (Nobukata et al., 1999). These results suggest that MPA itself and/or its metabolites might stimulate blood coagulation.

MPA exhibits low oral bioavailability (< 10%), which may be due to numerous factors, including metabolism in the intestinal mucosa and liver (Stockdale and Rostom, 1989). In fact, MPA has been shown to undergo extensive and rapid metabolism in humans (Stockdale and Rostom, 1989) and in experimental animals (Rautio et al., 1985). Recently, we reported that MPA was metabolized by cytochrome P450 3A4 (CYP3A4) in human liver microsomes (Kobayashi et al., 2000). This finding agrees with the observation reported by Ohtsu et al. (1998) that the plasma concentration of MPA was lower than that of MPA alone when dexamethasone (DEX), a CYP3A inducer (Pichard et al., 1990; Morris and Davila, 1996) or phenobarbital (PB), an inducer of CYP2B, CYP2C and CYP3A (Waxman and Azaroff, 1992) was coadministered with MPA in patients with breast cancer. Similarly, PB administered with MPA to rats greater decrease in the plasma concentration of MPA, while SKF525A (a CYP inhibitor) administered with MPA to rats caused a smaller decrease in the plasma concentration of MPA compared to that in the case of administration of MPA alone (Saarni et al., 1983). These results suggest that plasma decay of MPA depends mainly on the metabolism of MPA by CYP, although it is not clear which CYP isoform(s) is responsible for the metabolism of MPA in rats.

Since the metabolic products of MPA in rats have not been elucidated, we determined the metabolism of MPA as the disappearance of the parent drug from an incubation mixture, and identified the rat CYP isoforms involved in the CYP-catalyzed metabolism of MPA by using liver microsomes of DEX-, PB- or β-naphthoflavone (BNF, a CYP1A inducer; Daujat et al., 1992; Morris and Davila, 1996)-treated female rats, and microsomes from baculovirus-infected insect cells expressing individual rat CYP isoforms in the present study. Since CYP1A, CYP2B, CYP2C and CYP3A are major CYP isoforms in female rat liver, their probe activities or contents in liver microsomes were determined. Moreover, we examined the effects of SKF525A and PB on change in bleeding time by a single po administration of MPA in female rats to elucidate whether MPA itself or its metabolites stimulates blood coagulation.

Methods

Chemicals

MPA was obtained from Pharmacia-Upjohn (Tokyo, Japan). Prazepam and aminopyrine were obtained from Nippon Roche (Tokyo, Japan). Furafylline and sulfaphenazole were purchased from Daiichi Pure Chemicals (Tokyo, Japan). Ketoconazole was obtained from Janssen Pharmaceutica (Beerse, Belgium). 6β-Hydroxytestosterone was purchased from Ultrafine Chemicals (Manchester, UK). Formaldehyde standard solution was purchased from Kanto Chemicals (Tokyo, Japan). BNF, 7-benzyloxyresorufin, 7-ethoxyresorufin, methoxyresorufin, resorufin and SKF525A were purchased from Sigma (St. Louis, MO). Glucose-6-phosphate, glucose-6-phosphate dehydrogenase and $NADP^+$ were purchased from Oriental Yeast (Tokyo, Japan). DEX, PB, testosterone, HPLC-grade acetonitrile and methanol, and other regents were purchased from Wako Pure Chemical Industries (Osaka, Japan).

All recombinant rat CYPs expressed in insect cells (CYP1A2, CYP2A2, CYP2B1, CYP2C6, CYP2C13, CYP2D1, CYP3A1 and CYP3A2) were obtained from Gentest (Woburn, MA). All recombinant CYPs were coexpressed with rat NADPH-CYP oxydoreductase (OR). Recombinant CYP2A2, CYP2B1, CYP2C6, CYP2C13, CYP3A1 and CYP3A2 were coexpressed with cytochrome b_5. Control microsomes were from insect cells infected with wild-type baculovirus.

Animals

Female Wistar rats were purchased from Japan SLC (Shizuoka, Japan). The rats were maintained under conditions of controlled temperature and light, with access to food and water ad libitum. They were 5 weeks old for preparation of microsomes and 7 weeks old for experiments in vivo.

Rat liver microsomes

Animals were injected intraperitoneally with either PB (one injection/day, 100 mg/kg dissolved in saline, n = 3) or BNF (one injection/day, 25 mg/kg dissolved in corn oil, n = 3) for 4 consecutive days. One rat was treated with DEX (one injection/day, 200 mg/kg suspended in corn oil) for 2 days and was subsequently treated with reduced DEX (one injection of 100 mg/kg). Rats treated with saline (n = 3) or corn oil (n = 3) were used as controls. One day after the final treatment, rats were killed, and the livers were removed. The livers were immediately frozen and stored at − 80 °C.

Rat liver microsomes were prepared by differential centrifugation and were stored at − 80 °C until use. Protein concentrations were measured using a DC protein assay kit (Bio-Rad, Hercules, CA).

MPA metabolism in rat liver microsomes

Since the metabolic products of MPA in humans and rats has not been elucidated, microsomal activity for MPA metabolism was determined by measuring the disappearance rate of MPA from an incubation medium with rat liver microsomes as reported previously (Kobayashi et al., 2000). Briefly, the basic incubation medium contained 0.1 mg protein/mL of rat liver microsomes, 0.1 mM EDTA, 100 mM potassium phosphate buffer (pH 7.4), an NADPH-generating system (0.5 mM $NADP^+$, 2.0 mM glucose-6-phosphate, 1 IU/ml of glucose-6-phosphate dehydrogenase, and 4 mM $MgCl_2$), and 0.25 μM MPA, in a

final volume of 250 μL. MPA was added to the incubation mixture at a final acetonitrile concentration of 1%. The mixture was incubated at 37 °C for 0, 7, 15 and 30 min. After the reaction was stopped by adding 100 μL of cold acetonitrile, 50 μL of prazepam (0.25 μg/ml in methanol) was added as an internal standard. The mixture was centrifuged at 1700 × *g* for 20 min, and 100 μL of the supernatant was analyzed using a Hitachi HPLC system (Tokyo, Japan) consisting of an L-7100 pump, an L-7400 UV detector, an L-7200 autosampler, a D-7500 integrator, and a CAPCELL PAK C_{18} UG120 column (4.6 × 250 mm, 5 μm; Shiseido, Tokyo, Japan). The mobile phase consisted of 10 mM phosphate/acetonitrile (40/60, v/v) with a flow rate of 1.0 ml/min. The eluate was monitored at a wavelength of 240 nm. The disappearance amount of MPA in the medium incubated at 37 °C with microsomes in the presence of the NADPH-generating system was determined as percentage of the initial amount of MPA in the medium without incubation.

In a preliminary study, MPA less than 0.25 μM disappeared from the incubation mixture at a first-order rate. Therefore, we used 0.25 μM MPA as the substrate concentration to determine the disappearance amount of MPA throughout the study.

Intrinsic clearance of MPA

The intrinsic clearance of MPA in rat liver microsomes was estimated from the volume of incubation medium and elimination rate constant using the following equation: intrinsic clearance = elimination rate constant X volume of incubation medium. The elimination rate constant of MPA in the incubation medium was calculated by regression analysis of semilogarithmic plots.

Inhibition study

The effects of furafylline (an inhibitor of CYP1A; Newton et al., 1995), sulfaphenazole (an inhibitor of CYP2C; Newton et al., 1995) and ketoconazole (an inhibitor of CYP3A; Newton et al., 1995) on the disappearance of MPA at a substrate concentration of 0.25 μM were studied using liver microsomes prepared from untreated rats. The concentrations of inhibitors used were 0.1 and 1 μM for ketoconazole and 1 and 10 μM for furafylline and sulfaphenazole. All inhibitors were added to the incubation medium at a final acetonitrile concentration of 1%.

Assay with recombinant CYPs

Microsomes from baculovirus-infected insect cells expressing CYP1A2 (lot 1), CYP2A2 (lot 1), CYP2B1 (lot 2), CYP2C6 (lot 1), CYP2C13 (lot 1), CYP2D1 (lot 2), CYP3A1 (lot 1) and CYP3A2 (lot 1) were used. The reactions were carried out as described for the rat liver microsomal study. To examine the role of individual CYP isoforms involved in the metabolism of MPA, each of the recombinant CYPs (30 pmol of CYP/mL) described above was incubated with 0.25 μM MPA for 30 min at 37 °C, according to the procedure recommended by the supplier.

Other microsomal enzyme activities

The activities of 7-ethoxyresorufin *O*-deethylase (EROD) and 7-benzyloxyresorufin *O*-debenzylase (BROD) were determined by an HPLC-fluorescence method. 7-Ethoxyresorufin (5 μM) or 7-benzylox-

yresorufin (5 μM) was incubated with 0.05 mg protein/mL of microsomes at 37 °C for 5 min as described for the assay of MPA metabolism in rat liver microsomes. 7-Ethoxyresorufin and 7-benzyloxyresorufin were dissolved in dimethylsulfoxide and added to the incubation mixture at final dimethylsulfoxide concentrations of 1% and 0.5%, respectively. After reaction had been stopped by adding 100 μL of cold acetonitrile, 50 or 20 μL of methoxyresorufin (20 mM in dimethylsulfoxide) was added as an internal standard for EROD and BROD activities, respectively. The mobile phase consisited of 20 mM potassium sodium phosphate buffer (pH 7.4)/acetonitrile (45/55, v/v) containing 2.5 mM of tetra-*n*-octylammonium bromide with a flow rate of 1.0 mL/min. The eluent was monitored at an excitation wavelength of 530 nm and emission wavelength of 580 nm by using a model 821-FP fluorescence detector (Jasco, Tokyo, Japan). Testosterone (50 μM) was incubated with 0.05–0.1 mg protein/mL of microsomes for 7–15 min. Formed 6β-hydroxytestosterone was measured as described previously (Kobayashi et al., 2000).

CYP2C contents of rat liver microsomes were determined by SDS-polyacrylamide gel electrophoresis and immunoblotting as described by Laemmli (1970) and Guengerich et al. (1982), respectively. Goat anti-rat CYP2C11 antiserum (Daiichi Pure Chemicals) was used, and the immunoblots were developed using a VECTASTAIN ABC kit (Vector Laboratories, Burlingame, CA) and 3, 3'-diaminobenzidine. Anti-rat CYP2C11 antibodies reacted with CYP2C11, CYP2C6 and CYP2C13. Therefore, the CYPs that cross-reacted with anti-rat CYP2C11 antibodies are referred to as CYP2C. The intensities of the immunoblots were measured using a model GT-9600 scanner (EPSON, Tokyo, Japan) equipped with NIH Image/Gel Analysis Program (Ver. 1.61) adapted for Macintosh computers.

Effect of MPA on bleeding time

The bleeding time was measured by the method of Nobukata et al. (1999) with slight modification. In brief, animals anesthetized with diethylether were placed in a cage at a room temperature of 25—30 °C with their tails hanging down vertically. At the ventral part of the tail of each animal, an incision (5 mm long and 1 mm deep) was made without injuring the large vein or artery. Blood was carefully blotted every 15 s onto filter paper until the bleeding had stopped. To avoid circadian fluctuations in the bleeding time, all measurements were carried out between 10 and 12 in the morning. The bleeding time was measured before treatment and at 20 hr after treatment with MPA (100 mg/kg dissolved in 0.5% carboxymethyl cellulose, po). Changes from the bleeding time before dosing were calculated.

Effects of SKF525A and PB on change in bleeding time by MPA

To examine the effects of CYP modulators (i.e., inhibitor or inducer) on change in bleeding time after a single po administration of MPA, animals were pretreated with SKF525A (inhibitor of CYPs), PB (inducer of CYPs) or the vehicle alone.

The animals were divided into four groups (SKF525A-treatment group, control group for SKF525A, PB-treatment group and control group for PB). Rats were treated with SKF525A (n = 5, 100 mg/kg dissolved in saline, ip) or saline (n = 4, ip) 1 hr before and 5 hr after MPA treatment. Rats were treated with PB (n = 5, 100 mg/kg/day in saline, ip) or saline (n = 4, ip) for 4 days followed by MPA administered 24 hr after the last injection of PB (Scheme 1).

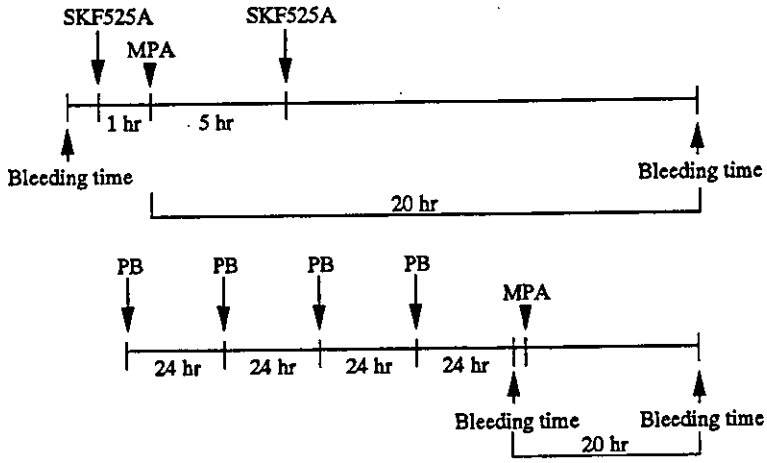

Scheme 1. Time-schedule for administration of drugs and measurement of bleeding time. The animals were divided into four groups (SKF525A-treatment group, control group for SKF525A, PB-treatment group and control group for PB). Rats were treated by po administration for MPA and ip administration for SKF525A and PB.

Statistical analyses

Results are expressed as means ± SD throughout the text. Student's *t*-test was used to analyze the significance of differences. A difference was regarded as statistically significant at the $p < 0.05$ level.

Results

CYP-dependent disappearance of MPA

When MPA (0.25 μM) was incubated with liver microsomes (0.1 mg protein/mL) prepared from an untreated rat for 15 min at 37 °C, disappearance of MPA in rat liver microsomes was found to be dependent on NADPH and was completely inhibited by SKF525A (1 mM), a typical CYP inhibitor (data not shown). These results suggest that the disappearance of MPA in rat liver microsomes is a CYP-dependent metabolic process.

Next, effects of chemical inhibitors of CYPs on the disappearance of MPA in liver microsomes prepared from an untreated rat were examined. Ketoconazole inhibited the disappearance of MPA in a concentration-dependent manner. The disappearance of MPA was inhibited to 34 and 3% of the control by 0.1 and 1 μM ketoconazole, respectively. Furaphylline (10 μM) inhibited the disappearance of MPA to 45% of the control, although the extent of inhibition was slight at a concentration of 1 μM (<25%). The inhibitory effect of sulfaphenazole on the disappearance of MPA was weak (<25%), even at a concentration of 10 μM.

Effects of CYP-inducers on intrinsic clearance of MPA

The intrinsic clearance of MPA in microsomes of a DEX-treated rat was 18-fold higher than that in microsomes of corn oil-treated rats (3.3 vs. 0.18 ± 0.04 mL/min/mg protein). The intrinsic clearance of

MPA in microsomes of PB-treated rats was 8-fold higher than that in microsomes of saline-treated rats (1.4 ± 0.26 vs. 0.15 ± 0.02 mL/min/mg protein, $p < 0.05$). There was no difference between the intrinsic clearance of MPA in microsomes of BNF-treated rats and in microsomes of corn oil-treated rats (0.24 ± 0.03 vs. 0.18 ± 0.04 mL/min/mg protein). As shown in Fig. 1, the intrinsic clearance of MPA in liver microsomes of rats treated with various CYP-inducers showed a significant correlation with testosterone 6β-hydroxylase activity ($r = 0.921$, $p < 0.001$). No other significant correlation was observed between the intrinsic clearance of MPA and EROD activity ($r = 0.270$), BROD activity ($r = 0.441$) or CYP2C contents ($r = 0.185$).

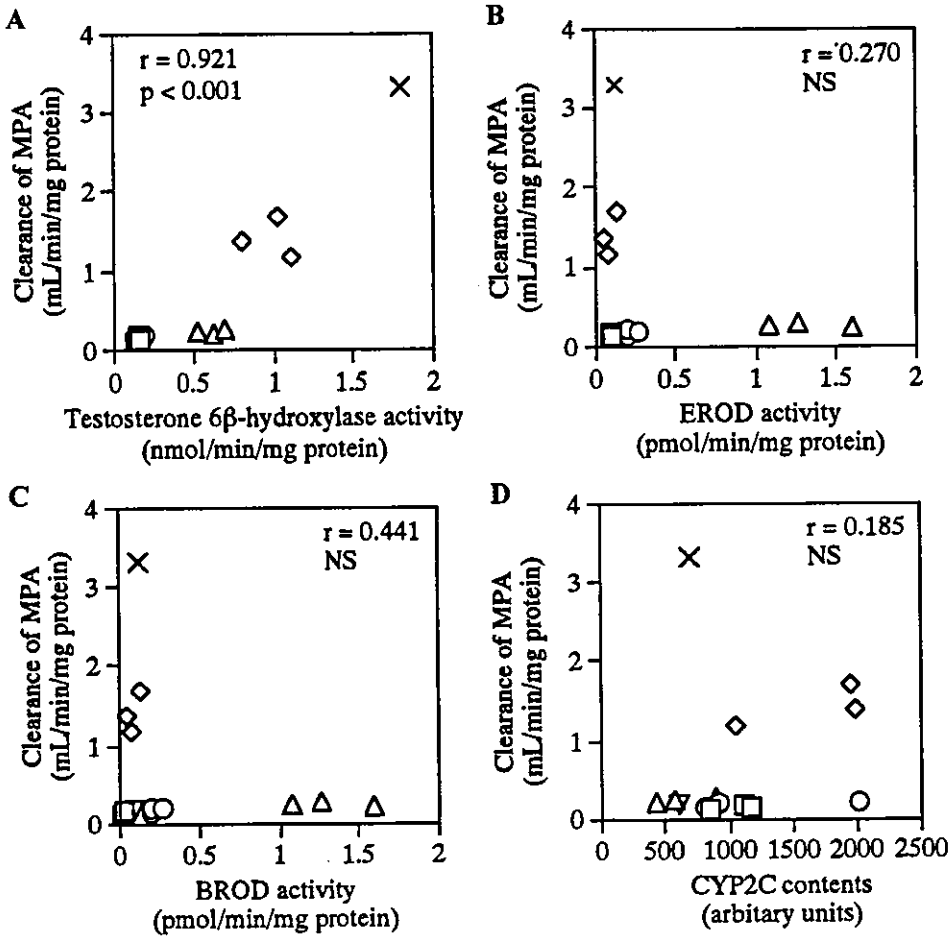

Fig. 1. Correlation of clearance of MPA with testosterone 6β-hydroxylase (A), EROD (B) and BROD activities (C) and CYP2C contents (D) in female rat liver microsomes. Microsomes were obtained from an untreated rat (▽, n = 1), and from rats treated with corn oil (○, n = 3), saline (□, n = 3), BNF (△, n = 3), PB (◇, n = 3) and DEX (×, n = 1). The protein concentration used for determining the clearance of MPA was 0.1 mg/mL in all cases except for 0.01 and 0.025 mg/mL for DEX- and PB-treated rats, respectively. Testosterone (50 μM) was incubated with 0.1 mg protein/mL of rat liver microsomes for 15 min. 7-Ethoxyresorufin (5 μM) and 7-benzyloxyresorufin (5 μM) were incubated with 0.05 mg protein/mL of rat liver microsomes for 5 min.

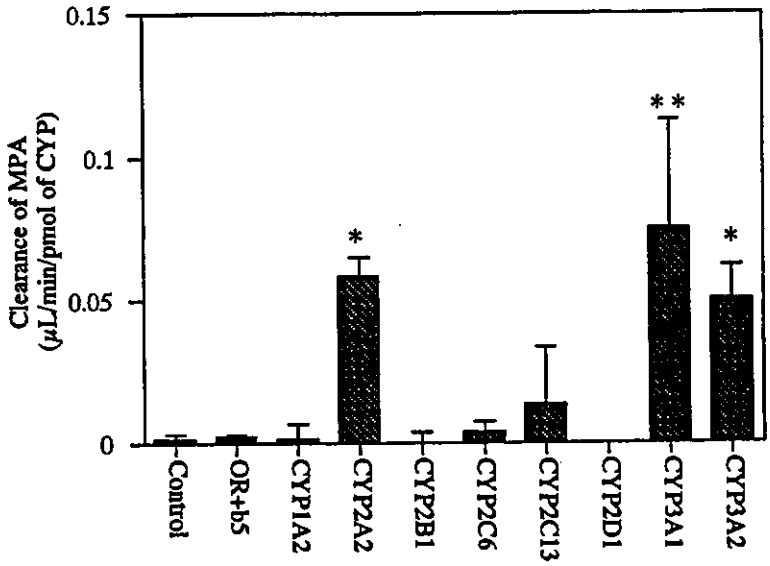

Fig. 2. Clearance of MPA in microsomes from baculovirus-infected insect cells expressing rat CYP1A2, CYP2A2, CYP2B1, CYP2C6, CYP2C13, CYP2D1, CYP3A1 and CYP3A2. MPA (0.25 μM) was incubated with microsomes (30 pmol of CYP/mL) at 37 °C for 30 min. Data are estimated from elimination rate constant of MPA in the incubation medium. Each column represents the mean ± SD of triplicate experiments. *p < 0.05; **p < 0.01 compared to microsomes expressing OR and b_5.

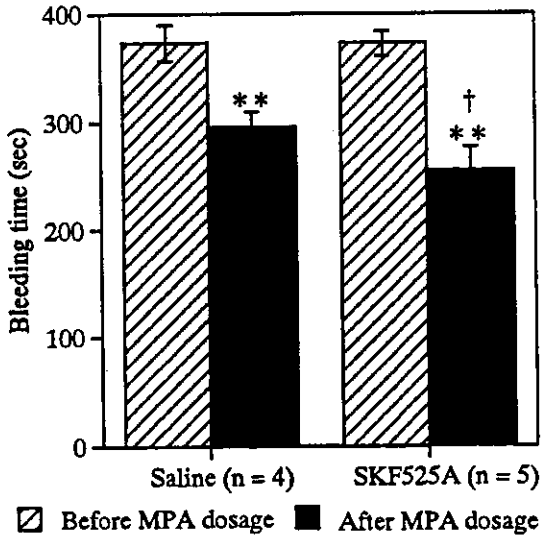

Fig. 3. Bleeding time before treatment (hatched bars) and at 20 hr after a single po administration of MPA (solid bars) in rats pretreated with saline or SKF525A. Rats were treated with MPA and SKF525A as described in Scheme 1. Each column represents the mean ± SD of data obtained from four or five rats. ** p < 0.01 compared with before MPA treatment, † p < 0.05 compared with the saline-treated group.

Study using recombinant rat CYPs

Microsomes from baculovirus-infected insect cells expressing CYP1A2, CYP2A2, CYP2B1, CYP2C6, CYP2C13, CYP2D1, CYP3A1 or CYP3A2 were examined in terms of the abilities of individual CYP isoforms to catalyze the metabolism of MPA (Fig. 2). Of the recombinant rat CYPs studied, CYP2A2, CYP3A1 and CYP3A2 showed remarkable disappearance of MPA by incubation. The clearance of MPA after incubation with CYP2A2, CYP3A1 and CYP3A2 were 0.059, 0.075 and 0.050 μL/min/pmol of CYP, respectively. CYP2C13 slightly showed the disappearance of MPA by incubation (0.013 μL/min/pmol of CYP). Control microsomes and the other recombinant CYPs exhibited no significant activity.

Effect of SKF525A on change in bleeding time by MPA treatment

As shown in Fig. 3, MPA significantly shortened the bleeding time at 24 hr after a single po administration in both the groups of saline-treated (373 ± 17 to 296 ± 14 sec, $p < 0.01$) and SKF525A-treated rats (372 ± 11 to 255 ± 23 sec, $p < 0.01$). The shortening effect of MPA on the bleeding time in the SKF525A-treated group was significantly stronger than that in the saline-treated group (−117 ± 20 vs. −77 ± 7 sec, $p < 0.05$).

Effect of PB on change in bleeding time by MPA treatment

As shown in Fig. 4, MPA significantly shortened the bleeding time at 24 hr after a single po administration in rats pretreated with saline (426 ± 20 to 351 ± 36 sec, $p < 0.01$). On the other hand, in the rats pretreated with PB, MPA did not cause any significant change in the bleeding time (395 ± 31 to 393 ± 39 sec).

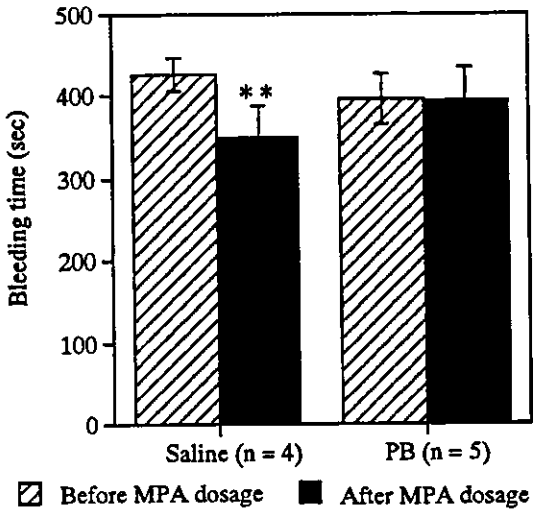

Fig. 4. Bleeding time before treatment (hatched bars) and at 20 hr after a single po administration of MPA (solid bars) in rats pretreated with saline or PB. Rats were treated with MPA and PB as described in Scheme 1. Each column represents the mean ± SD of data obtained from four or five rats. ** $p < 0.01$ compared with that before MPA treatment.

Discussion

The results of the present study suggest that CYP3A is the principal enzyme responsible for the CYP-catalyzed metabolism of MPA in liver microsomes of female rats. The supporting evidence can be summarized as follows. First, intrinsic clearance of MPA in liver microsomes of female rats was induced by DEX and PB, CYP3A inducers (Fig. 1). Second, the intrinsic clearance of MPA in liver microsomes of female rats treated with various CYP-inducers was highly correlated with testosterone 6β-hydroxylase activity (Fig. 1). Third, ketoconazole (1 μM), an inhibitor of CYP3A, potently inhibited the disappearance of MPA in rat liver microsomes. Fourth, a significant disappearance of MPA was observed in cDNA-expressed CYP3A1 and CYP3A2 (Fig. 2).

In the present study, the disappearance of MPA in rat liver microsomes was inhibited by furaphylline (an inhibitor of CYP1A) and sulfaphenazole (an inhibitor of CYP2C) to 45% and 25% of the control, respectively. However, intrinsic clearance of MPA in liver microsomes of female rats was not induced by BNF, a potent CYP1A inducer (Fig. 1). In addition, no disappearance of MPA was observed in cDNA-expressed CYP1A2 (Fig. 2). Therefore, the contribution of CYP1A to the overall metabolism of MPA in rat liver microsomes appears to be negligible. On the other hand, slight disappearance of MPA was observed in cDNA-expressed CYP2C13 (Fig. 2), whereas the intrinsic clearance of MPA in liver microsomes of female rats treated with various CYP-inducers was not correlated with CYP2C contents (Fig. 1). The results suggest that CYP2C might be involved in the CYP-catalyzed metabolism of MPA in rat liver microsomes as minor enzymes.

The present study using cDNA-expressed CYPs showed that a remarkable disappearance of MPA occurred not only in the presence of CYP3A but also in the presence of CYP2A2 (Fig. 2). This finding indicates that MPA is a substrate of these isoforms. On the other hand, it is well known that the expression of the constitutive forms in rats depends on sex (Pampori and Shapiro, 1999). Since CYP3A2 and CYP2A2 are male-specific isoforms, these isoforms are not likely to be principal enzymes responsible for the CYP-catalyzed metabolism of MPA in liver microsomes of female rats.

Although PB is a typical CYP2B inducer, no increase of BROD activity in microsomes was observed after PB treatment in the present study. At the present time, we have no idea because of limited induction studies using female rats. However, Yoshinari et al. (2001) reported that PB induced CYP2B1 mRNA in male WKY (Wistar Kyoto) rats but not female rats. Induction of *CYP2B1* gene by PB might be also sexually dimorphic in Wistar rats.

SKF525A is well known as a typical inhibitor of CYP. Saarni et al. (1983) reported that SKF525A administered with MPA caused a smaller decrease in the plasma concentration of MPA compared with that in the case of administration of MPA alone in rats. In this study, oral administration of MPA significantly shortened the bleeding time in both the groups of saline-treated and SKF525A-treated rats. The shortening effect of MPA on bleeding time in the SKF525A-treated group was significantly stronger than that in the saline-treated group (Fig. 3). These results suggest that metabolism of MPA mainly catalyzed by CYP3A1 in female rats was inhibited by SKF525A and that the metabolic inhibition of CYP3A1 by SKF525A caused an increase in plasma concentration of MPA, which resulted in enhancement of MPA-induced hypercoagulation.

Although oral administration of MPA significantly shortened the bleeding time in saline-treated rats, MPA did not cause any significant change in the bleeding time in PB-treated rats (Fig. 4). As shown in Fig. 1, the intrinsic clearance of MPA in microsomes of PB-treated rats was higher than that in the control rats. In addition, PB administered with MPA caused a greater decrease in the plasma concentration of

MPA compared with that in the case of administration of MPA alone in rats (Saarni et al., 1983). These findings suggest that metabolism of MPA mainly catalyzed by CYP3A1 in female rats was induced by PB and that the metabolic induction of CYP3A1 by PB caused a decrease in the plasma concentration of MPA, which resulted in reduction of MPA-induced hypercoagulation.

Although the results of the present study suggested that MPA itself but not CYP-dependent metabolite(s) is responsible for MPA-induced hypercoagulation, it is possible that MPA metabolite(s) formed via non-CYP enzyme is responsible for the blood coagulation in vivo. This is because bioavailability of orally administered MPA (i.e., via intestinal CYP3A) may be influenced by SKF525A and PB. However, first metabolic process of MPA appears to be mainly dependent on CYP, since intraperitoneally administered ^{3}H-MPA was rapidly changed to polar metabolites in PB-treated rats, while the production of these metabolites decreased in SKF525A-treated rats (Saarni et al., 1983). Therefore, we assumed that MPA itself rather than MPA metabolites is a predominant factor being responsible for the effects of MPA administration on bleeding time in vivo and its effect was influenced by CYP-dependent metabolism of MPA.

Conclusion

The results of the present study using in vitro and in vivo techniques suggested that the CYP-catalyzed metabolism of MPA is mainly catalyzed by CYP3A1 in liver microsomes of female rats and that the MPA-induced hypercoagulation in female rats is induced by MPA itself. Since MPA is metabolized by CYP3A4 in humans (Kobayashi et al., 2000), decreased capacity of CYP3A4 may be one of the factors causing an increase in the plasma concentration of MPA itself, which results in MPA-induced thrombosis.

References

Daujat, M., Peryt, B., Lesca, P., Fourtanier, G., Domergue, J., Maurel, P., 1992. Omeprazole, an inducer of human CYP1A1 and 1A2, is not a ligand for the Ah receptor. Biochemical and Biophysical Research Communications 188 (2), 820–825.

Etienne, M.C., Milano, G., Frenay, M., Renee, N., Francois, E., Thyss, A., Schneider, M., Namer, M., 1992. Pharmacokinetics and pharmacodynamics of medroxyprogesterone acetate in advanced breast cancer patients. Journal of Clinical Oncology 10 (7), 1176–1182.

Guengerich, F.P., Wang, P., Davidson, N.K., 1982. Estimation of isozymes of microsomal cytochrome P-450 in rats, rabbits, and humans using immunochemical staining coupled with sodium dodecylsulfate-polyacrylamide gel electrophoresis. Biochemistry 21 (5), 1698–1706.

Kobayashi, K., Mimura, N., Fujii, H., Minami, H., Sasaki, Y., Shimada, N., Chiba, K., 2000. Role of human cytochrome P450 3A4 in metabolism of medroxyprogesterone acetate. Clinical Cancer Research 6 (8), 3297–3303.

Laemmli, U.K., 1970. Cleavage of structural proteins during the assembly of the head of bacteriophage T4. Nature 227 (259), 680–685.

Morris, D.L., Davila, J.C., 1996. Analysis of rat cytochrome P450 isoenzyme expression using semi-quantitative reverse transcriptase-polymerase chain reaction (RT-PCR). Biochemical Pharmacology 52 (5), 781–792.

Newton, D.J., Wang, R.W., Lu, A.Y.H., 1995. Cytochrome P450 inhibitors. Evaluation of specificities in the in vitro metabolism of therapeutic agents by human liver microsomes. Drug Metabolism and Disposition 23 (1), 154–158.

Nobukata, H., Katsuki, Y., Ishikawa, T., Inokuma, M., Shibutani, Y., 1999. Effect of dienogest on bleeding time, coagulation, fibrinolysis, and platelet aggregation in female rats. Toxicology Letters 104 (1–2), 93–101.

Ohtsu, T., Fujii, H., Wakita, H., Igarashi, T., Itoh, K., Imoto, S., Kohagura, M., Sasaki, Y., 1998. Pharmacokinetic study of low- versus high-dose medroxyprogesterone acetate (MPA) in women. Cancer Chemotherapy Pharmacology 42 (1), 1–8.

Pampori, N.A., Shapiro, B.H., 1999. Gender differences in the responsiveness of the sex-dependent isoforms of hepatic P450 to the feminine plasma growth hormone profile. Endocrinology 140 (3), 1245–1254.

Pichard, L., Fabre, I., Fabre, G., Domergue, J., Saint Aubert, B., Mourad, G., Maurel, P., 1990. Cyclosporin A drug interactions. Screening for inducers and inhibitors of cytochrome P-450 (cyclosporin A oxidase) in primary cultures of human hepatocytes and in liver microsomes. Drug Metabolism and Disposition 18 (5), 595–606.

Rautio, A., Saarni, H.U., Arranto, A.J., Stengard, J.H., Karki, N.T., Sotaniemi, E.A., 1985. Metabolism of medroxyprogesterone acetate and hepatic drug metabolism activity. Research Communications in Chemical Pathology and Pharmacology 47 (2), 305–308.

Rosendaal, F.R., 1999. Venous thrombosis: a multicausal disease. Lancet 353 (9159), 1167–1173.

Saarni, H.U., Rautio, A., Karki, N.T., Sotaniemi, E.A., 1983. Disposition of medroxyprogesterone acetate and drug metabolism. Research Communications in Chemical Pathology and Pharmacology 39 (2), 251–260.

Stockdale, A.D., Rostom, A.Y., 1989. Clinical significance of differences in bioavailability of medroxyprogesterone acetate preparations. Clinical Pharmacokinetics 16 (3), 129–133.

Waxman, D.J., Azaroff, L., 1992. Phenobarbital induction of cytochrome P-450 gene expression. Biochemical Journal 281 (3), 577–592.

Yoshinari, K., Sueyoshi, T., Moore, R., Negishi, M., 2001. Nuclear receptor CAR as a regulatory factor for the sexually dimorphic induction of CYP2B1 gene by phenobarbital in rat livers. Molecular Pharmacology 59 (2), 278–284.

Comprehensive *UGT1A1* Genotyping in a Japanese Population by Pyrosequencing, *Mayumi Saeki,[1] Yoshiro Saito,[1,2*] Hideto Jinno,[1,3] Masahiro Tohkin,[4] Kouichi Kurose,[1,4] Nahoko Kaniwa,[1,4] Kazuo Komamura,[5,6] Kazuyuki Ueno,[7] Shiro Kamakura,[5] Masafumi Kitakaze,[5] Shogo Ozawa,[1,8] and Jun-ichi Sawada[1,2]* ([1] Project Team for Pharmacogenetics, [2] Division of Biochemistry and Immunochemistry, [3] Division of Environmental Chemistry, [4] Division of Medicinal Safety Science, and [8] Division of Pharmacology, National Institute of Health Sciences, 1-18-1, Kamiyoga, Setagaya-ku, Tokyo 158-8501, Japan; [5] Division of Cardiology, [6] Department of Cardiovascular Dynamics Research Institute, and [7] Department of Pharmacy, National Cardiovascular Center, 5-7-1, Fujishirodai, Suita, Osaka 565-8565, Japan; * address correspondence to this author at: Division of Biochemistry and Immunochemistry, National Institute of Health Sciences, 1-18-1, Kamiyoga, Setagaya-ku, Tokyo 158-8501, Japan; fax 81-3-3707-6950, e-mail yoshiro@nihs.go.jp)

Glucuronidation, catalyzed by UDP-glucuronosyltransferases (UGTs), is important in the detoxification and enhanced elimination of a large number of endogenous and exogenous substrates. The human *UGT1A* gene complex contains at least nine variations of exon 1, common exons 2–5, and a single exon 1 splices to exons 2–5 *(1)*.

Of the UGT1A isoforms, UGT1A1 is primarily responsible for the glucuronidation of bilirubin in the human liver and can also conjugate phenols, anthraquinones, flavonoids, and a variety of therapeutic drugs and their metabolites (e.g., SN-38, an active irinotecan metabolite) *(2, 3)*. Several functional polymorphisms in *UGT1A1* are associated with reduced bilirubin glucuronidation activity and cause hyperbilirubinemia (Gilbert and Crigler–Najjar syndromes).

UGT1A1 TATA box variants [$A(TA)_6TAA>A(TA)_{5/7/8}$ TAA] are associated with enhanced [$(TA)_5$] or reduced [$(TA)_{7/8}$] *UGT1A1* transcription *(4)*. Among them, the $(TA)_6$ and $(TA)_7$ repeats have been reported in Asians. The variant $(TA)_7$ is associated with reduced glucuronidation of SN-38 and bilirubin, as well as the pathogenesis of Gilbert syndrome *(5)*. In addition, a T-to-G substitution at nucleotide −3279 (A of the translational start codon in GenBank accession no. AF297093.1 is nucleotide number 1) in the *UGT1A1* phenobarbital-responsive enhancer module reduces transcriptional activity *(6)*.

The most common nonsynonymous single-nucleotide polymorphism (SNP) (211G>A) that causes an amino acid alteration (glycine to arginine at codon 71) is found in Asian populations at frequencies of 13–23% *(7, 8)*. The 686C>A (P229Q) variation in the Taiwanese has a frequency of 2.8% *(8)*. Also associated with Gilbert syndrome are 211G>A (G71R) and 686C>A (P229Q). Rare in Japanese and Taiwanese patients is 1456T>G (Y486D), which is associated with the more severe type II Crigler–Najjar syndrome *(8, 9)*. Our previous study demonstrated that the in vitro intrinsic clearance (V_{max}/K_m) of SN-38 was decreased to 47% for G71R, 52% for P229Q, and 5% for Y486D compared with that of the wild type *(10)*. Recently, a novel SNP, 247T>C (F83L), was shown to be associated with Gilbert syndrome patients in Thailand. This variation was also found in the Japanese at a frequency of 1.4% *(11)*.

The detection of genotypic differences in the coding and promoter regions of this enzyme thus is important for understanding the metabolism of various compounds and for clinical diagnosis. Several methods have been reported for genotyping the TA repeat polymorphism *(4, 5)*, but no single method has been available for simultaneous genotyping of all known polymorphisms. DNA sequencing is the most accurate and informative technique, but is time-consuming. Other high-throughput genotyping methods, such as PCR-restriction fragment length polymorphism analysis, Taq-Man, and matrix-assisted laser desorption/ionization time-of-flight mass spectrometry, are not completely suitable for typing repeat polymorphisms.

Pyrosequencing is a real-time, nonelectrophoretic method for DNA sequencing that is based on enzymatic reactions catalyzed by ATP sulfurylase and luciferase. The inorganic pyrophosphates that are released after deoxynucleotide incorporation are monitored. Unreacted nucleotides are degraded by apyrase, allowing iterative nucleotide addition. It has been shown that SNP typing can be efficiently performed by pyrosequencing *(12)*.

In this study, we developed a method for genotyping the common *UGT1A1* polymorphisms [−3279T>G, TA repeat, 211G>A (G71R), 247T>C (F83L), 686C>A (P229Q), and 1456T>G (Y486D)]. DNA was extracted from the blood leukocytes of 48 Japanese patients who had been administered beta blockers. The ethics committees of the National Cardiovascular Center and the National Institute of Health Sciences approved this study. Written informed consent was obtained from all participants.

The genotypes of the 48 patients were determined by pyrosequencing and compared with direct sequencing results. For pyrosequencing, fragments were directly amplified from genomic DNA (10–15 ng) by Ex-Taq (1 U; Takara Shuzo) with specific amplification primer pairs (either primer was biotinylated; Table 1). The PCR conditions were 94 °C for 5 min, followed by 50 cycles of 94 °C for 30 s, 58 °C for 45 s, and 72 °C for 30 s.

Biotinylated single-stranded DNA fragments were generated by the following procedure at room temperature. PCR products were mixed with Streptavidin-Sepharose High Performance (Amersham Biosciences AB) in Binding Buffer (2×; 10 mmol/L Tris-HCl, 1 mmol/L EDTA, 2 mol/L NaCl, 1 mL/L Tween 20, pH 7.6) for 10 min. The beads were transferred to a MultiScreen-HV Plate (Millipore Corporation), and the Binding Buffer was removed by application of reduced pressure. DNA attached to the beads was denatured for 1 min in 50 μL of Denaturation Buffer (0.2 mol/L NaOH) and washed twice with 150 μL of Wash Buffer (10 mmol/L Tris acetate, pH 7.6). The beads were suspended in 50 μL of Annealing Buffer (20 mmol/L Tris acetate, 2 mmol/L magnesium acetate, pH 7.6) and transferred to the 96-well PSQ plate (Pyrosequencing AB); 10 pmol of the sequencing primer (poly-

Table 1. Primers for *UGT1A1* amplification, pyrosequencing, and direct sequencing.

A. Pyrosequencing

		Polymorphism	Primer name	Sequence, 5′ to 3′
Amplification		−3279T>G	UGTCAR1stF3	TTAACCAAAGAACATTCTAACGG
			b1A1CAR-R5[a]	b-TGCTGTTCCCCAAACTTC
		TA repeat	bTATA-F[a]	b-TCCCTGCTACCTTTGTGGAC
			UGT1A1-TATA-R	GAGGTTCGCCCTCTCCTACT
		211G>A (G71R), 247T>C (F83L)	bG71R-F[a]	b-CAGCAGAGGGGACATGAAAT
			G71R-R	CAAAAACATTATGCCCGAGAC
		686C>A (P229Q)	UGT1A1b-Left	TTTCTGTGCGACGTGGTTTA
			bP229Q-R[a]	b-GGGCCTAGGGTAATCCTTCA
		1456T>G (Y486D)	bExon5F-Y486D[a]	b-TGGGTGGAGTTTGTGATGA
			exon5-R	CCTTATTTCCCACCCACTT
Sequencing	Forward	−3279T>G	1A1CAR-SeqF	CCAAGGGTAGAGTTCAGT
	Reverse	TA repeat	UGT1A1-TATA-SeqR	TCGCCCTCTCCTACTTATAT
	Reverse	211G>A (G71R)	UGT1A1-G71R-seqR	TTCAAGGTGTAAAATGCTC
	Reverse	247T>C (F83L)	F83L-SeqR	ACATCCTCCCTTTGGA
	Forward	686C>A (P229Q)	UGT1A1-229SeqF	GACGTGGTTTATTCCC
	Reverse	1456T>G (Y486D)	Exon5-1456R	CGTCCAAGGAATGGT

B. Sequencing

		Amplified region and polymorphism to be detected		Primer name	Sequence, 5′ to 3′
First amplification	Forward			UGT1A1CAR-Ex5ZF	GGTGGTGGGAGTGAGTTTAGT
	Reverse			UGT1A1CAR-Ex5ZR	AGAGGGAAATAGTGGACAGAA
Second amplification	Forward	−3279T>G and surrounded sequence		UGTCAR1stF2	AAGAACATTCTAACGGTTCATAA
	Reverse	−3279T>G and surrounded sequence		UGTCAR1stR2	TGAATCATTGCATCGGCTGCCCA
	Forward	Exon 1		UGT1A11stF	TATCTCTGAAAGTGAACTCCCTG
	Reverse	Exon 1		UGT1A11stR	GCACACAGAGTAAAATGTCCAA
	Forward	Exon 5		UGT1AEx5-F5-2	CTGGGCAACACAATAAGACCT
	Reverse	Exon 5		UGT1AEx5-1stR	CTCAAATACACCACCCACCAA
Sequencing	Forward		−3279T>G	UGTCAR1stF2	AAGAACATTCTAACGGTTCATAA
	Reverse		−3279T>G	CAR-Rseq2	TGCCCACCTGAATAAACCCCACC
	Forward		211G>A (G71R), 247T>C (F83L)	UT1A11F1	GAACCTCTGGCAGGAGCAAAG
	Reverse		TA repeat	UTT1A1R3-2	ATGCCCGAGACTAACAAAAGAC
	Forward			UT1A11F4	ATCAGAGACGGAGCATTTTACACC
	Reverse	Exon 1	211G>A (G71R), 247T>C (F83L)	UT1A11R4	CACGTAGGAGAATGGGTTGGG
	Forward		686C>A (P229Q)	UT1A11F5	AGTACCTGTCTCTGCCCAC
	Reverse		686C>A (P229Q)	UT1A11R5	AGTGGATTTTGGTGAAGGCAG
	Forward			UT1A11F6	TGCTCATTGCCTTTTCACAG
	Reverse			UGT1A1seqR1-2	TCAGATACCAAGAAATCATCCA
	Reverse			UGT1AEx5-R5-2	ACCTTTGAATCCCGCACTC
	Forward	Exon 5	1456T>G (Y486D)	UGT1AEx5seqF1	GTTTGGAAAATCTGGTAGTCTTC
	Forward			UGT1AEx5seqF2	AAATGTTGTGCTTATGGCTACC
	Reverse		1456T>G (Y486D)	UGT1AEx5seqR1	TCTTGGATTTGTGGGCTTTCT

[a] Biotinylated primer.

acrylamide gel electrophoresis-purified grade; Table 1) for SNP analysis was then added to the single-stranded fragments. The mixture was incubated at 95 °C for 2 min, and then cooled to room temperature for annealing. An automated pyrosequencing instrument, the PSQ™ 96MA (Pyrosequencing AB), and the PSQ 96 SNP reagent set (Pyrosequencing AB) were used for genotyping. The total procedure for 96 samples took ~4 h, including ~25 min to run the samples. In addition, direct sequencing was performed as described previously, using the primers listed in Table 1 *(13)*. The time required for the entire sequencing procedure for 96 samples was ~12 h, including ~3 h of run time on the ABI Prism 3700 DNA Analyzer (Applied Biosystems).

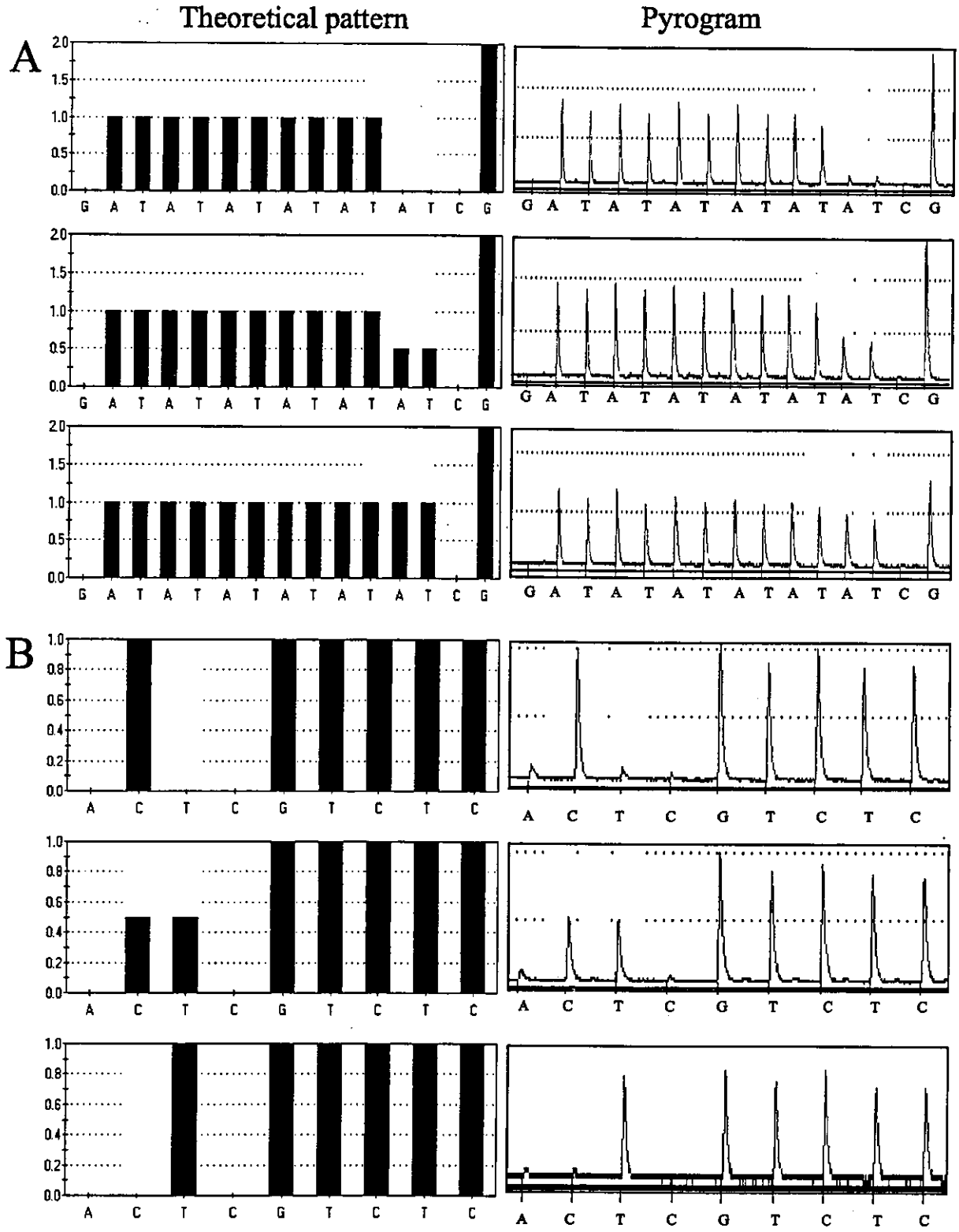

Fig. 1. Pyrograms for the *UGT1A1* TA repeat $(TA)_6$>$(TA)_7$ (*A*) and 211G→A (G71R; *B*).

The actual pyrograms are shown on the *right*, and the theoretical patterns from the pyrosequencing software are shown on the *left*. (*A*), the sequence to be analyzed is underlined in TTATATATATATATA[TA]TGG (antisense strand corresponding to CCA[TA]TATATATATATAATAA). In the 1st (*G*) and 14th (*C*) bp, unrelated nucleotides were added to estimate background values. (*Top*), homozygous $(TA)_6/(TA)_6$; (*middle*), heterozygous $(TA)_6/(TA)_7$; (*bottom*), homozygous $(TA)_7/(TA)_7$. For $(TA)_7/(TA)_7$, DNA samples derived from established cell lines were used because no homozygous variants were found in the examined patients. (*B*), the sequence to be analyzed is C/TGTCTC (antisense strand corresponding to GAGACG/A). In the 1st (*A*) and 4th (*C*) bp, unrelated nucleotides were added to estimate the background. (*Top*), homozygous C/C; (*middle*), heterozygous C/T; (*bottom*), homozygous T/T.

Two polymorphisms in the promoter region (−3279T>G and TA repeat) and four additional SNPs that lead to reduced activity [211G>A (G71R), 247T>C (F83L), 686C>A (P229Q), and 1456T>G (Y486D)] were analyzed. All samples were successfully genotyped at all polymorphic sites. The genotyping results were identical to those obtained by direct sequencing. Fig. 1 shows representative sequencing patterns (pyrograms) for the *UGT1A1* TA repeat $(TA)_6$>$(TA)_7$ (Fig. 1A) and 211G>A (G71R; Fig. 1B). DNA samples derived from established cell lines or in vitro-mutated cDNA plasmids were also used as templates for the genotypes that were not detected, such as the homozygous $(TA)_7$ repeat, heterozygous and homozygous 247T>C (F83L), homozygous 686C>A (P229Q), and heterozygous and homozygous 1456T>G (Y486D). Correct genotyping results were successfully obtained from these control samples (data for the TA repeat are shown). This genotyping method was also applicable to the other TA repeat variants, $(TA)_5$ and $(TA)_8$, which have been found in African Americans, with the same primers and only a slight modification to the sequencing program (data not shown).

The allelic frequencies of these polymorphisms were 0.281 for −3279T>G (4 homozygous G/G and 19 heterozygous T/G patients), 0.135 for $(TA)_6$>$(TA)_7$ (13 heterozygous 6/7 repeat patients) and 211G>A (G71R; 2 homozygous A/A and 9 heterozygous G/A patients), and 0.010 for 686C>A (P229Q; 1 heterozygous C/A patient), respectively. These frequencies were similar to those reported previously *(4, 6–8)*. Two low-frequency SNPs, 247T>C (F83L) and 1456T>G (Y486D) *(9, 11)*, were not detected in this study. We also did not find any Japanese patients with the $(TA)_5$ or $(TA)_8$ repeat.

In summary, we developed a pyrosequencing-based genotyping method for six functionally significant polymorphisms that are especially important in the Japanese. The pyrosequencing data were identical to those obtained from direct sequencing. Pyrosequencing thus can expedite studies on the association between genetic polymorphisms and pharmacokinetic or clinical data.

This study was supported in part by the Program for Promotion of Fundamental Studies in Health Sciences (MPJ-3 and MPJ-6) of the Organization for Pharmaceutical Safety and Research (OPSR) of Japan and the Program for Promotion of Studies in Health Sciences of the Ministry of Health, Labor and Welfare.

References

1. Gong Q-H, Cho JW, Huang T, Potter C, Gholami N, Basu NK, et al. Thirteen UDP glucuronosyltransferase genes are encoded at the human UGT1 gene complex locus. Pharmacogenetics 2001;11:357–68.
2. Senafi SB, Clarke DJ, Burchell B. Investigation of the substrate specificity of a cloned expressed human bilirubin UDP-glucuronosyltransferase: UDP-sugar specificity and involvement in steroid and xenobiotic glucuronidation. Biochem J 1994;303:233–40.
3. Iyer L, King CD, Whitington PF, Green MD, Roy SK, Tephly TR, et al. Genetic predisposition to the metabolism of irinotecan (CPT-11). Role of uridine diphosphate glucuronosyltransferase isoform 1A1 in the glucuronidation of its active metabolite (SN-38) in human liver microsomes. J Clin Invest 1998;101:847–54.
4. Beutler E, Gelbart T, Demina A. Racial variability in the UDP-glucuronosyltransferase 1 (UGT1A1) promoter: a balanced polymorphism for regulation of bilirubin metabolism? Proc Natl Acad Sci U S A 1998;95:8170–4.
5. Monaghan G, Ryan M, Seddon R, Hume R, Burchell B. Genetic variation in bilirubin UDP-glucuronosyltransferase gene promoter and Gilbert's syndrome. Lancet 1996;347:578–81.
6. Sugatani J, Yamakawa K, Yoshinari K, Machida T, Takagi H, Mori M, et al. Identification of a defect in the UGT1A1 gene promoter and its association with hyperbilirubinemia. Biochem Biophys Res Commun 2002;292:492–7.
7. Akaba K, Kimura T, Sasaki A, Tanabe S, Ikegami T, Hashimoto M, et al. Neonatal hyperbilirubinemia and mutation of the bilirubin uridine diphosphate-glucuronosyltransferase gene: a common missense mutation among Japanese, Koreans and Chinese. Biochem Mol Biol Int 1998;46:21–6.
8. Huang CS, Luo GA, Huang MJ, Yu SC, Yang SS. Variations of the bilirubin uridine-diphosphoglucuronosyl transferase 1A1 gene in healthy Taiwanese. Pharmacogenetics 2000;10:539–44.
9. Aono S, Yamada Y, Keino H, Hanada H, Nakagawa T, Sasaoka Y, et al. Identification of defect in the genes for bilirubin UDP-glucuronosyltransferase in a patient with Crigler-Najjar syndrome type II. Biochem Biophys Res Commun 1993;197:1239–44.
10. Jinno H, Tanaka-Kagawa T, Hanioka N, Saeki M, Ishida S, Nishimura T, et al. Glucuronidation of 7-ethyl-10-hydroxycamptothecin (SN-38), an active metabolite of irinotecan (CPT-11), by human UGT1A1 variants, G71R, P229Q, and Y486D. Drug Metab Dispos 2003;31:108–13.
11. Sutomo R, Laosombat V, Sadewa AH, Yokoyama N, Nakamura H, Matsuo M, et al. Novel missense mutation of the UGT1A1 gene in Thai siblings with Gilbert's syndrome. Pediatr Int 2002;44:427–32.
12. Ahmadian A, Gharizadeh B, Gustafsson AC, Sterky F, Nyren P, Uhlen M, et al. Single-nucleotide polymorphism analysis by pyrosequencing. Anal Biochem 2000;280:103–10.
13. Saeki M, Ozawa S, Saito Y, Jinno H, Hamaguchi T, Nokihara H, et al. Three novel single nucleotide polymorphisms in UGT1A10. Drug Metab Pharmacokinet 2002;17:488–90.